Executive dysfunction relates to salience network desegregation in behavioral variant frontotemporal dementia

Melanie A. Matyi[1], Hamsanandini Radhakrishnan[1], Christopher A. Olm[1], Jeffrey S. Phillips[1], Philip A. Cook[2], Emma Rhodes[1], James C. Gee[2], David J. Irwin[1], Corey T. McMillan[1] & Lauren Massimo[1,3]*

[1]Penn Frontotemporal Degeneration Center, Department of Neurology, School of Medicine, University of Pennsylvania, Philadelphia; [2]Penn Imaging and Computing Science Laboratory, University of Pennsylvania, Philadelphia; [3]Department of Biobehavioral Health Sciences, School of Nursing, University of Pennsylvania, Philadelphia

Corresponding Author: Lauren Massimo, PhD, 3700 Hamilton Walk, B603 Richards Medical Laboratories, Philadelphia, PA 19104 (lmassimo@upenn.edu).

Abstract

Network segregation, which facilitates functional specialization of cognition in healthy brains, breaks down with neurodegeneration and therefore is a candidate biomarker of disease. However, limited evidence exists evaluating the role of network desegregation in behavioral variant frontotemporal degeneration (bvFTD), especially the breakdown of structural networks and the impact of this process on cognition. We collected neuropsychological tests of executive function (digit span backwards, letter fluency, category fluency) and a control task (confrontation naming), and diffusion MRI data in a sample of 95 bvFTD patients without evidence of primary progressive aphasia and 72 age-matched cognitively normal controls (CNC). We evaluated the hypotheses that bvFTD would have desegregation in structural networks compared to CNC and that, in bvFTD, executive dysfunction would relate to desegregation of the salience network. Probabilistic tractography maps were generated from diffusion MRI, and network segregation was defined as greater within-network connectivity than between-network connectivity. One-way ANCOVAs tested for group differences in network desegregation. Then linear regressions examined associations between network desegregation and neuropsychological test performance. Analyses controlled for age, sex, education, mean cortical atrophy, motion during diffusion MRI scan, imaging protocol, and disease duration. Compared to CNC, patients with bvFTD exhibited desegregation of the salience ($p < .001$) and global brain network ($p = .006$). In bvFTD, desegregation of salience network was associated with worse executive function ($p_{corrected} = .039$) but not confrontation naming. Results demonstrate associations between executive dysfunction and salience network desegregation in patients with bvFTD. Our findings indicate that brain network desegregation, reflecting reduced neural capacity for specialized processing, may contribute to the emergence of executive dysfunction in bvFTD.

Introduction

Behavioral variant frontotemporal degeneration (bvFTD) is a common cause of early-onset neurodegenerative disease (Seltman & Matthews, 2012) characterized by significant behavioral changes and executive dysfunction. bvFTD is a network disorder, with selective vulnerabilities in the salience network early on in the bvFTD disease course, followed by the frontoparietal executive control network (Seeley et al., 2009). The salience network is instrumental in orchestrating coordinated brain network activation (Menon & Uddin, 2010; Seeley, 2019). For example, salience network coordinates engagement and deactivation of the executive control network to facilitate responses to emotionally relevant stimuli, functions that are clearly linked with socioemotional processes (Seeley, 2019). The majority of prior work examining the clinical consequences of network breakdown in bvFTD have examined behavioral, rather than executive, consequences. Indeed, reduced functional connectivity of the salience network is associated with impairments in social cognition such as apathy (Godefroy et al., 2022), decreased socioemotional sensitivity (Toller et al., 2018) and interpersonal warmth (Toller et al., 2019). Because much of this prior work has investigated functional networks, the role of *structural* network connectivity in bvFTD is unclear. Structural connectivity reflects the capacity of the network to facilitate functional connectivity, as white matter pathways form the underlying structure that enables dynamic and synchronized functional activity (Baum et al., 2020; Honey et al., 2010). Therefore, in this current study we examined structural brain networks.

As reflected in bvFTD criteria (Rascovsky et al., 2011), the core symptoms of bvFTD include behavioral impairment and executive dysfunction. Executive function is related to the dorsolateral prefrontal and cingulate cortices, among other regions (Ardila et al., 2018). Indeed,

there is some evidence that executive dysfunction in bvFTD is related to reduced integrity of the cingulum (Tartaglia et al., 2012) and atrophy of related regions, including the cingulate gyrus, inferior and middle frontal cortex, and insula (Lagarde et al., 2013), suggesting there are multiple regions necessary in order to facilitate executive function. These regions associated with executive dysfunction in bvFTD overlap with the salience and frontoparietal control networks (Yeo et al., 2011). Thus, the breakdown of salience and frontoparietal control networks in bvFTD may be related to executive dysfunction in bvFTD, however, the executive consequences of network breakdown are understudied. To date, the few studies that have examined functional network connectivity in relation to executive functioning in bvFTD find that poorer performance on executive function tasks are related to lower or disrupted functional connectivity. Indeed, poor verbal fluency is associated with lower integration of frontal cortex functional connectivity and lower global functional connectivity (Filippi et al., 2017; Rittman et al., 2019) and the executive domain of the Frontal Assessment Battery is associated with resting state functional connectivity of the default mode network (Trojsi et al., 2015). This prior work is informative and is indicative of complex relationships between executive dysfunction and brain connectivity, however these studies relied on small samples of bvFTD patients, functional connectivity, and/or examination of the brain as a whole or of singular regions associated with large-scale brain networks.

Network neuroscience approaches have established that brain networks support complex cognitive functions. Prior work has established that, during development, children have undifferentiated intrinsic networks and that over the course of the lifespan they become segregated in predictable ways, initially increasing in adolescence and then declining in aging (Baum et al., 2017; Chan et al., 2014; He et al., 2020). Indeed, there is an emerging literature on the importance of modular segregation of intrinsic networks that support specialization of

cognition (Baum et al., 2017) while at the same time reducing interference among network systems, and that with neurodegeneration, networks become less segregated and increasingly merged into a less differentially organized network. A common metric of network differentiation is system segregation (Chan et al., 2014), which reflects the balance of connectivity within a network to connectivity between a network and the rest of the brain network. Moreover, reduced segregation (i.e., less functional specialization or de-differentiation) is predictive of reduced cognitive performance in healthy older adults and in Alzheimer's disease (Chan et al., 2014; Ewers et al., 2021). However, network de-differentiation and its consequences on executive dysfunction in bvFTD has not been examined. Therefore, our study is novel because we examine the executive consequences of structural network desegregation in a relatively large sample of patients with bvFTD.

The current study examines the cognitive consequences of structural network de-differentiation in bvFTD. Given evidence that the salience network is targeted early on in the bvFTD disease course and the frontoparietal control network is targeted later on in disease (Seeley et al., 2009), we hypothesized that the salience network, and possibly the frontoparietal control network, would be desegregated in bvFTD patients compared to cognitively normal controls (CNC) and would predict poorer performance on tests of executive function.

Methods

Participants

A total of 95 patients with a clinical diagnosis of bvFTD without evidence of primary progressive aphasia (PPA) were included in this study. All patients were initially evaluated at the University of Pennsylvania Frontotemporal Degeneration Center by experienced clinicians using published consensus criteria for bvFTD (Rascovsky et al., 2011). Participants and their legal

representatives participated in an informed consent procedure approved by the Institutional Review Board at the University of Pennsylvania. All participants had diffusion MRI (dMRI) data that successfully completed preprocessing procedures detailed below, and neuropsychological testing within 9 months of dMRI scan. For patients with multiple sessions (i.e., multiple timepoints with both dMRI and neuropsychological data) meeting these criteria, the session with the lowest mean framewise displacement, a measure of motion during the dMRI scan, was included in analyses. We studied 72 age-matched heathy controls with a normal cognitive exam and no history or neurologic or psychiatric condition.

Cognitive assessments

To evaluate the hypothesized role of the salience and frontoparietal control networks in executive dysfunction, we used a composite score of three verbally-mediated measures of executive functioning. We also examined a control measure involving lexical retrieval with minimal executive resource demands.

The executive function composite was defined as the average z-score of phonemic fluency, category-guided fluency and backward digit span (Lezak et al., 2012). The two measures of verbal fluency (i.e., phonemic- and category-guided fluency) involve mental search and working memory which are two dimensions of executive function. Backward digit span requires planning, mental manipulation of information, and working memory, all dimensions of executive function. To obtain z-scores, norms derived from the National Alzheimer's Coordinating Center (NACC) Uniform Data Set (UDS) version 3 were applied (Weintraub et al., 2018). These standardized scores facilitated averaging across the 3 executive function tests. For the phonemic fluency test, patients are given 60 seconds to generate as many unique words as possible, excluding proper nouns and numbers, starting with the letter "F". The score is the total number

of correct, non-repeated responses given in 60 seconds. For the category-guided fluency test, patients are given 60 seconds each to generate as many unique words as possible for animals and vegetables. Scores for animals and vegetables were averaged after z-scoring except when only one test was administered. Lastly, for backward digit span, patients are read a series of digits and are then asked to repeat the digits in reverse order. Trials increase in the length of the digit sequence until the patient makes consecutive errors. The score is the digit sequence length of the last successful trial.

We additionally examined performance on a control measure, confrontation naming. Confrontation naming is a task involving picture naming that relies largely on semantic knowledge and less on executive resources. Visual confrontation naming was assessed with the 30-item version of the Boston Naming Test (BNT) or the Multilingual Naming Test (MINT). Patients are asked to name pictures and are given as much time as possible to respond. NACC UDS version 2 (Weintraub et al., 2009) and version 3 (Weintraub et al., 2018) norms were applied to BNT and MINT scores, respectively, as BNT was administered in UDS2 and MINT was administered in UDS3.

Neuroimaging Acquisition

Participants underwent MRI an average of 1.3 months with a range of 0 (same day) to 8.9 months from neuropsychological testing. Both dMRI and structural T1 weighted (T1w) MPRAGE MRI were collected with one of three protocols described below. All dMRI protocols collected 30 non-collinear directions at b=1000 s/mm^2 with at least one b0 volume using single-shot, spin-echo, diffusion-weighted echo planar imaging with fat saturation. All images were acquired on a 3.0 Tesla SIEMENS TIM Trio scanner. Protocol was included as a covariate in all analyses.

Protocol A: dMRI data was collected with the following parameters: FOV = 245x245; matrix size = 112x112; number of slices = 57; voxel size = 2.1875x2.1875x2.2 mm3; TR = 6700ms; TE = 85ms. T1w data was collected using an 8 channel head coil, axial plane with repetition time = 1620 ms, echo time = 3.87 ms, slice thickness = 1.0 mm, flip angle = 15 degrees, matrix = 192 × 256, and in-plane resolution = 0.977 × 0.977 mm.

Protocol B: dMRI data was collected with the following parameters: FOV = 240x240; matrix size = 128x128; number of slices = 70; voxel size = 1.875x1.875x2.0 mm3; TR = 8100ms; TE = 83ms. T1w data was collected as described in Protocol A.

Protocol C: dMRI data was collected as described in Protocol B. T1w data was collected using a 64 channel head coil, sagittal plane with repetition time = 2300 ms, echo time = 2.95 ms, slice thickness = 1.2 mm, flip angle = 0 degrees, matrix = 256 × 240, and in-plane resolution = 1.05 × 1.05 mm.

Neuroimaging Analysis

dMRI data were preprocessed and reconstructed with QSIPrep 0.21.4, which is based on Nipype 1.8.6 (Gorgolewski et al., 2011) (RRID:SCR_002502). Many internal operations of QSIPrep use Nilearn 0.10.1 (Abraham et al., 2014) (RRID:SCR_001362) and Dipy (Garyfallidis et al., 2014). MP-PCA denoising as implemented in MRtrix3's dwidenoise (Veraart et al., 2016) was applied with a 5-voxel window. Gibbs unringing was then performed using MRtrix3's mrdegibbs (Kellner et al., 2016). B1 field inhomogeneity was corrected using dwibiascorrect from MRtrix3 with the N4 algorithm (Tustison et al., 2010). FSL's eddy was used for head motion correction and eddy current correction (Andersson & Sotiropoulos, 2016) with outlier replacement (Andersson et al., 2016). Scans were not acquired with reverse phase-encode blips so synb0 was implemented to generate an undistorted non-diffusion weighted image (Schilling et

al., 2019). Outputs of synb0 were fed into FSL's TOPUP (Andersson et al., 2003) to estimate and remove susceptibility-induced off-resonance fields. The TOPUP-estimated fieldmap was incorporated into the eddy current and head motion correction interpolation. Final interpolation was performed using the jac method. Framewise displacement (FD) using the implementation in Nipype, following the definitions by (Power et al., 2014) were calculated based on the preprocessed DWI. The DWI time-series were resampled to ACPC, generating a preprocessed DWI run in ACPC space with 1.5mm isotropic voxels.

Multi-tissue fiber response functions were estimated using the Dhollander algorithm (Dhollander et al., 2016, 2019). FODs were estimated via constrained spherical deconvolution (CSD) (Tournier et al., 2004, 2008) using an unsupervised multi-tissue method (Dhollander et al., 2016, 2019). A single-shell-optimized multi-tissue CSD (Tournier et al., 2004) was performed using MRtrix3Tissue (https://3Tissue.github.io), a fork of MRtrix3 (Tournier et al., 2019). FODs were intensity-normalized using mtnormalize (Raffelt et al., 2017). Whole-brain probabilistic tractography was performed using the tckgen function with second-order integration over FODs. Streamline count after Spherical-deconvolution Informed Filtering of Tractograms (SIFT) (Smith et al., 2013) was applied to the Schaefer 100 parcellation of the 7-network Yeo intrinsic brain networks (Schaefer 100x7) (Schaefer et al., 2018; Yeo et al., 2011) and used as our measure of structural connectivity. In the Schaefer 100x7 parcellation each region is assigned to one of seven networks, salience (or ventral attention), frontoparietal control, default mode, dorsal attention, visual, somatomotor, and limbic.

To extract cortical thickness measures, T1w data were processed using the Advanced Normalization Tools (ANTs) antsCorticalThickness.sh pipeline (Tustison et al., 2014) (https://github.com/ftdc-picsl/antsct-aging [v0.3.3-p01]). Briefly, intensity nonuniformity was

corrected with N4 bias correction (Tustison et al., 2010). Atropos segmentation used template-based priors to divide images into 6 classes (cortical gray matter (GM), subcortical GM, white matter (WM), cerebrospinal fluid (CSF), brainstem, and cerebellum) (Avants et al., 2011). Labels from the Schaefer 100x7 parcellation (Schaefer et al., 2018; Yeo et al., 2011) were transformed from Oasis template space to native space by using the warps made with antsCorticalThickness, and were masked by individual cortex defined using voxel-wise thickness > 0.0001 mm.

Network differentiation

Network differentiation was measured using system segregation which characterizes differentiation as greater within-network connectivity than between-network connectivity following the equation as previously described (Chan et al., 2014):

$$\text{System segregation} = \frac{mean\ within\ network - mean\ between\ network}{mean\ within\ network\ connectivity},$$

where within-network connectivity is the mean connectivity among regions within a given network and between-network connectivity is the mean connectivity between a given network and all other networks. Thus, higher system segregation values reflect stronger network differentiation, where within network connectivity is greater than between network connectivity. In contrast, lower system segregation values reflect network de-differentiation, where within-network connectivity is more balanced with, or less than, between-network connectivity. In order to test our hypotheses, we performed statistical tests on system segregation for the salience and frontoparietal control networks, in addition to global segregation, which is the mean segregation of all seven Yeo networks (i.e., salience/ventral attention, frontoparietal control, default mode, dorsal attention, visual, somatomotor, and limbic).

Statistical Methods

Descriptive statistics were calculated for demographic and clinical variables, using chi-squared tests for categorical variables and t-tests with unequal variances assumption for continuous variables. T-tests were also performed to evaluate gray matter differences between the patient and control groups.

ANCOVA models evaluated the influence of group (patient vs. control) on global segregation and of the salience and frontoparietal control networks, adjusted for age at MRI scan, sex, education, mean framewise displacement (FD) during dMRI scan, MRI protocol, and global cortical thickness. Next, linear models evaluated the association of system segregation of global, salience and frontoparietal control networks on an executive function composite including digit span backwards, letter-guided fluency, and category-guided fluency, as well as our control task, confrontation naming. All models adjusted for disease duration, age at MRI scan, sex, education, dMRI scan mean FD, MRI protocol, and global cortical thickness. Reported p-values were adjusted using false discovery rate (FDR) correction.

Results

Demographic variables

The bvFTD and control groups did not differ on age at MRI scan, education, or MRI protocol (see Table 1). The bvFTD patients had greater motion on dMRI scans ($t = 4.30$, $df = 138.34$, $p < .001$) and were more likely to identify as male $\chi^2 = 13.8$, $df = 1$, $p < .001$). We also report means and standard deviations of neuropsychological testing after standardization.

Table 1. Sample Characteristics

	bvFTD	Controls	difference
N	95	72	
Age	62.7 (8.00)	61.4 (9.36)	n.s.
Motion	.48 (.30)	.33 (.14)	$p < .001$
Education	16.1 (3.1)	15.9 (2.3)	n.s.
Sex (%F)	33.7%	63.9%	$p<.001$
Protocol (A/B/C)	18/71/6	14/57/1	n.s.
Disease duration	4.56 (2.66)	--	
Animal fluency	-1.90 (1.1)	--	
Vegetable fluency	-1.89 (.97)	--	
Category fluency	-1.90 (.98)	--	
Digit span backwards	-1.14 (1.2)	--	
Executive function composite	-1.58 (.92)	--	
Confrontation naming	-1.65 (2.2)	--	

Note. Standardized z-scores are reported for all neuropsychological tests. Values in parentheses are standard deviations unless otherwise noted.

Cortical atrophy in bvFTD patients

Patients with bvFTD exhibited greater atrophy in most brain regions, with the greatest degree of atrophy in the frontal and temporal regions as expected. There was one area of the left visual cortex where there was no difference between bvFTD patients and control participants. Figure 1 illustrates the magnitude of cortical thickness differences between groups (Mowinckel & Vidal-Piñeiro, 2020).

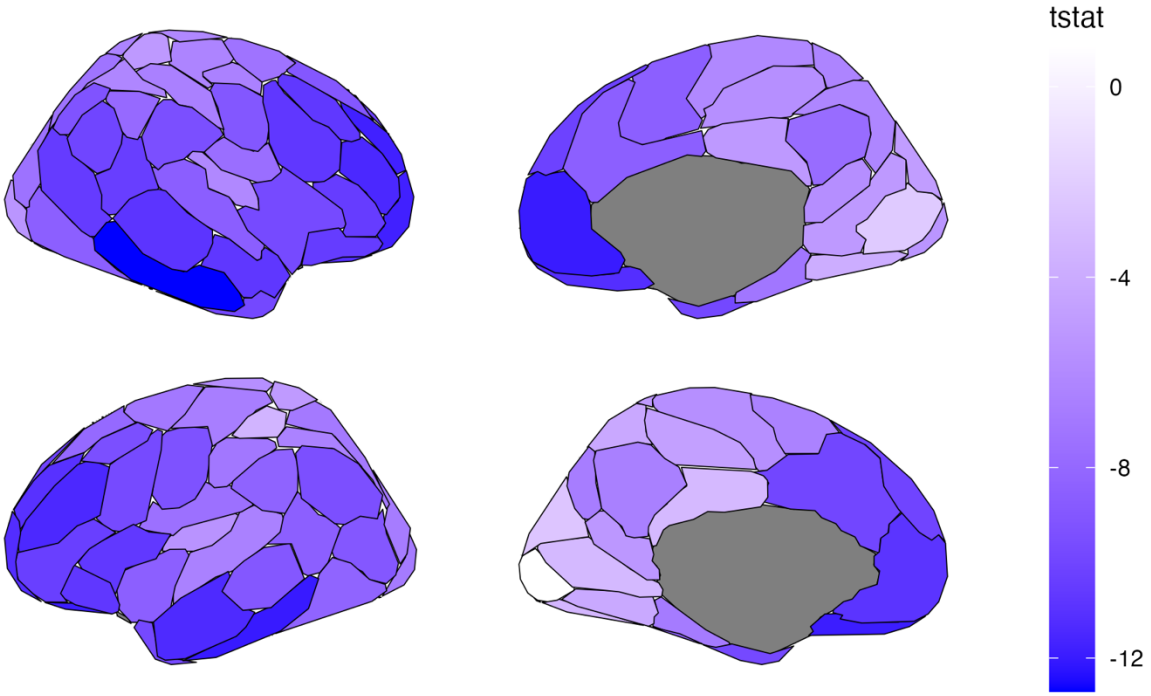

Figure 1. Cortical atrophy in bvFTD patients compared to control participants

Desegregation of intrinsic brain networks in bvFTD patients compared to control participants

ANCOVA comparisons evaluated network desegregation of the salience and frontoparietal control networks, in addition to global brain network desegregation. As illustrated in Figure 2, we observed a significant difference between patients with bvFTD and control participants in salience desegregation ($F(1, 158) = 18.91$, $p < .001$) and global desegregation ($F(1, 158) = 7.61$, $p = .006$). We did not observe differences in the frontoparietal control network ($F(1, 158) = 1.85$, $p = .176$).

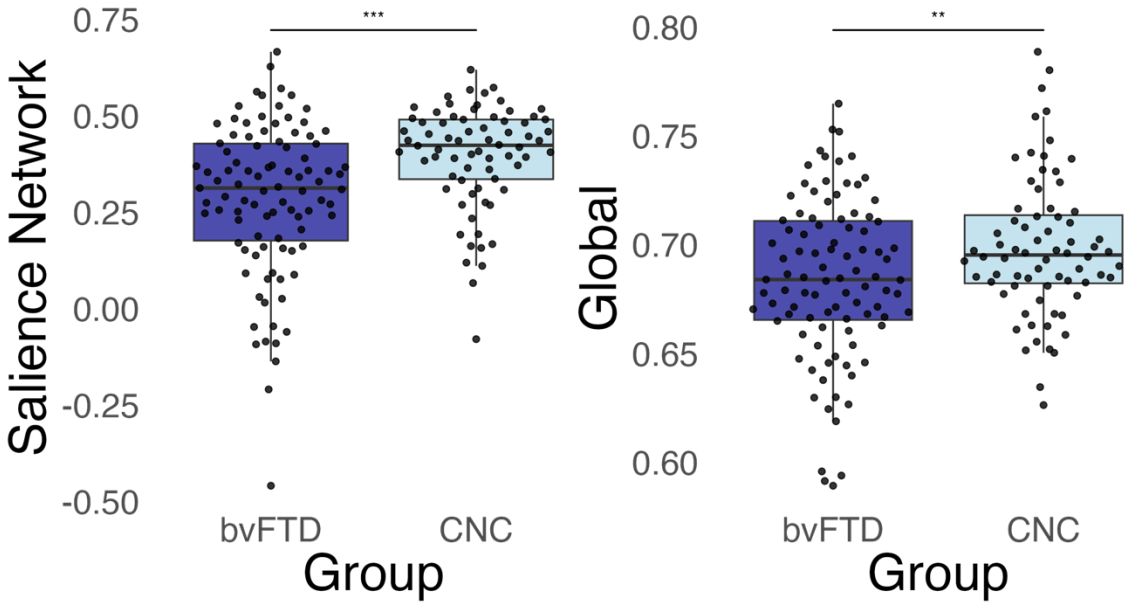

Figure 2. The salience network and global network are desegregated in bvFTD patients compared to cognitively normal controls (CNC). $^{**}p < .01$; $^{***}p < .001$

Desegregation of intrinsic brain networks in bvFTD patients relates to executive dysfunction

Linear regressions evaluated whether salience network, frontoparietal control network and global network desegregation was predictive of executive function. Salience network desegregation was associated with poorer performance across tests of executive functioning (β = 1.19, SE = 0.42, $p_{corrected}$ = .039). Associations between salience network desegregation and the executive function tests making up the composite score are reported in the supplement (Fig. S1, Table S1). As predicted, we did not observe any associations between network desegregation and confrontation naming (Figure 3). Global and frontoparietal control network desegregation were not associated with performance on any of the examined neuropsychological tests, suggesting that executive dysfunction is specific to desegregation of the salience network.

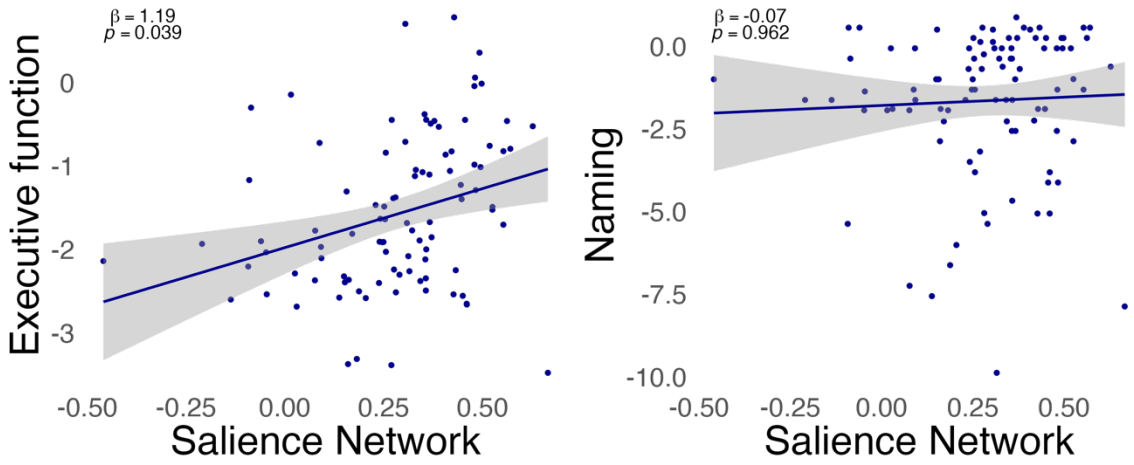

Figure 3. Desegregation of the salience network is associated with executive dysfunction but not confrontation naming in bvFTD patients. Standardized z-scores of neuropsychological test performance are shown.

Discussion

In the current study, we examined the contribution of network desegregation to executive dysfunction in bvFTD. Results demonstrate that poorer performance across neuropsychological tests with high executive demands (i.e., digit span, phonemic and category fluency) but not low executive demands (i.e., confrontation naming) are associated with desegregation of the salience network. Since structural brain network desegregation reflects the reduced capacity of the brain to support specialized processing, current findings suggest a potential mechanism for the emergence of executive dysfunction in bvFTD. Critically, analyses controlled for cortical atrophy, and thus, salience network desegregation is a unique contributor to executive dysfunction in bvFTD, above and beyond cortical atrophy.

The salience network, also referred to as the ventral attention network, is important for facilitating socioemotional processes, and thus, prior work in bvFTD has focused on relating loss of salience network integrity to deficits in socioemotional processes (e.g., Toller et al., 2018).

Expanding upon prior work, our findings demonstrate the executive dysfunction consequences related to salience network degradation. The observed relationship between executive dysfunction and salience network desegregation may be related to the critical role the salience network plays in facilitating coordinated activation and deactivation of other large-scale networks, including the frontoparietal control network (Goulden et al., 2014). Our results, highlighting the role of desegregation of salience, but not frontoparietal control network, suggest that the executive dysfunction observed in bvFTD may result from the lack of recruitment, rather than direct dysfunction, of the frontoparietal control network by the salience network. In other words, we suggest that *structural* desegregation of the salience network may contribute to inefficient, or lack of, recruitment of the frontoparietal control network in response to task demands, resulting in poor performance on tasks requiring high executive demand. Future work should investigate this by assessing the interaction of structural and functional network dynamics between the intrinsic networks.

Dynamic *functional* connectivity analyses indicate that dynamic segregation and integration, and the ability to switch between these states is associated with cognitive abilities, as measured by a cognitive composite score and, in particular, processing speed (Wang et al., 2021). Specifically, longer switch times between segregated and integrated states, and less time spent in a segregated state are associated with poorer performance on executive tasks. Here we examined structural connectivity and suggest a possible mechanism for prior evidence of associations between functional connectivity dynamics and cognitive functioning. One possibility for longer switch times between segregated and integrated states may be the breakdown of salience network structure which, in turn, may prevent the salience network from facilitating efficient switching of states. Therefore, a breakdown in salience network structure may result in a downstream impact

of poor recruitment of other functional networks, together resulting in executive dysfunction. Indeed, results from prior work, utilizing functional connectivity, suggests that cognitive decline is related to less selective recruitment of brain networks during cognitive tasks (He et al., 2020). The identification of similar patterns of network desegregation at the level of the structural brain network in the present study, as have previously been observed with functional networks, adds to current network hypotheses of executive dysfunction in bvFTD. Our findings further suggest that executive dysfunction is related to the breakdown of the brain structure supporting functional networks, beyond cortical atrophy.

Much of the prior research examining the re-organization and degradation of brain networks in bvFTD have leveraged functional MRI and functional connectivity analysis (Ferreira et al., 2022). Here, we leverage structural connectivity to examine how the capacity of brain networks to facilitate coordinated activity supports executive functioning. Present findings, derived from diffusion MRI, demonstrate that breakdown in network configurations, analogous to those observed in functional networks, exist at the structural level. Evidence of the breakdown of structural networks underlying functional networks has implications for how functional connectivity findings are interpreted. Together, prior functional, and current structural, connectivity findings suggest that structural network breakdown impacts the ability of functional networks to be recruited. Future work should examine coupling of dMRI with fMRI to assess the extent to which structural network desegregation explains functional network dynamics, particularly in the context of executive dysfunction and neuropsychiatric symptoms in bvFTD.

The present study demonstrates that structural network desegregation in bvFTD has consequences for executive dysfunction. This adds to extant research which has focused on network contributions to socioemotional dysfunction in bvFTD. Critically, our finding of the

selective impact of salience network desegregation on executive dysfunction indicate that the consequences of salience network desegregation extend beyond socioemotional processes. Furthermore, salience network desegregation contributed to executive dysfunction above and beyond whole brain cortical atrophy, indicating that desegregation explains additional variance in executive dysfunction beyond cortical atrophy. In other words, preserved salience network structure may attenuate the effect of cortical atrophy on executive dysfunction, similar to findings in Alzheimer's disease (Ewers et al., 2021). The links between salience network integrity and executive function demonstrated here should be further explored, as salience network desegregation may represent a mechanism for cognitive decline in bvFTD. Alternatively, preserved segregation, or differentiation, of the salience network in bvFTD patients may represent resilience to pathology.

Strengths of this study include inclusion of cortical atrophy in our models. Although atrophy explains a portion of variance in executive function, salience desegregation remains a significant predictor after controlling for atrophy. Furthermore, we demonstrate specificity in our findings. Salience desegregation, but not global desegregation, was related to executive dysfunction, and was not related to performance on a confrontation naming/lexical retrieval task. In an additional effort to demonstrate the specificity of salience desegregation to executive dysfunction, we excluded bvFTD patients with symptoms of primary progressive aphasia to reduce the potential impact of language impairments on findings.

The strengths of this study should be considered in light of some limitations. First, although the study benefits from a large sample of patients with bvFTD, analyses were based on structural networks calculated from 30 direction dMRI data, and thus our data are limited by low angular resolution. Second, MRI data was pooled across highly similar, but different protocols.

Third, our patient sample was characterized only by clinical phenotype; different underlying proteinopathies and biofluid biomarkers were not considered. Additionally, our sample is highly homogeneous in regards to demographic makeup, with the majority of participants identifying as white and highly educated. Lastly, this study utilized a cross-sectional design, and thus, we are unable to make any conclusions about the direction of effect between network desegregation and executive function deficits.

In summary, structural network desegregation may represent a mechanism of executive dysfunction in bvFTD. Alternatively, preserved salience network segregation, despite cortical atrophy, may reflect resilience to cognitive decline in bvFTD. Future work should examine the association of executive dysfunction and network desegregation longitudinally to assess whether network desegregation predicts executive dysfunction and to tease out structure-function network dynamics that may contribute to cognitive decline. The identification of biological mechanisms underlying the process of network desegregation will provide more insights to inform symptom management in bvFTD by suggesting modifiable mechanisms to target. Furthermore, network desegregation in bvFTD may also reflect cognitive reserve, suggesting mechanisms of cognitive resilience in bvFTD. In Alzheimer's disease, evidence of preserved segregation as a reflection of cognitive resilience exists: at similar disease severity, patients with greater segregation had better than expected cognition (Ewers et al., 2021). Future work should examine interactions of disease stage and network desegregation in relation to executive dysfunction in bvFTD.

Conclusion

We demonstrate that the structural integrity of the salience network is compromised in bvFTD patients compared to control participants, in line with prior findings highlighting salience network dysfunction in bvFTD. We further show the executive consequences of structural

desegregation of the salience network in bvFTD patients. Reduced differentiation, as measured by lower segregation, of the salience network in bvFTD patients, relates to poorer performance on neuropsychological evaluation of executive function. Because structural brain network desegregation reflects the reduced capacity of the brain network to support specialized processing, current findings suggest a potential mechanism for the emergence of executive dysfunction in bvFTD. Critically, all analyses controlled for cortical atrophy, and thus, salience network desegregation is a unique contributor to executive dysfunction in bvFTD. This assessment of structural network organization provides insight into the brain architecture that contributes to executive dysfunction in bvFTD; structural brain network desegregation, reflecting reduced neural capacity for specialized processing, may mediate emergence of executive dysfunction in bvFTD.

References

Abraham, A., Pedregosa, F., Eickenberg, M., Gervais, P., Mueller, A., Kossaifi, J., Gramfort, A., Thirion, B., & Varoquaux, G. (2014). Machine learning for neuroimaging with scikit-learn. *Frontiers in Neuroinformatics*, *8*. https://doi.org/10.3389/fninf.2014.00014

Andersson, J. L. R., Graham, M. S., Zsoldos, E., & Sotiropoulos, S. N. (2016). Incorporating outlier detection and replacement into a non-parametric framework for movement and distortion correction of diffusion MR images. *NeuroImage*, *141*, 556–572. https://doi.org/10.1016/j.neuroimage.2016.06.058

Andersson, J. L. R., Skare, S., & Ashburner, J. (2003). How to correct susceptibility distortions in spin-echo echo-planar images: Application to diffusion tensor imaging. *NeuroImage*, *20*(2), 870–888. https://doi.org/10.1016/S1053-8119(03)00336-7

Andersson, J. L. R., & Sotiropoulos, S. N. (2016). An integrated approach to correction for off-resonance effects and subject movement in diffusion MR imaging. *NeuroImage*, *125*, 1063–1078. https://doi.org/10.1016/j.neuroimage.2015.10.019

Ardila, A., Bernal, B., & Rosselli, M. (2018). Executive functions brain system: An activation likelihood estimation meta-analytic study. *Archives of Clinical Neuropsychology*, *33*(4), 379–405. https://doi.org/10.1093/arclin/acx066

Avants, B. B., Tustison, N. J., Wu, J., Cook, P. A., & Gee, J. C. (2011). An open source multivariate framework for n-tissue segmentation with evaluation on public data. *Neuroinformatics*, *9*(4), 381–400. https://doi.org/10.1007/s12021-011-9109-y

Baum, G. L., Ciric, R., Roalf, D. R., Betzel, R. F., Moore, T. M., Shinohara, R. T., Kahn, A. E., Vandekar, S. N., Rupert, P. E., Quarmley, M., Cook, P. A., Elliott, M. A., Ruparel, K., Gur, R. E., Gur, R. C., Bassett, D. S., & Satterthwaite, T. D. (2017). Modular segregation

of structural brain networks supports the development of executive function in youth. *Current Biology*, *27*(11), Article 11. https://doi.org/10.1016/j.cub.2017.04.051

Baum, G. L., Cui, Z., Roalf, D. R., Ciric, R., Betzel, R. F., Larsen, B., Cieslak, M., Cook, P. A., Xia, C. H., Moore, T. M., Ruparel, K., Oathes, D. J., Alexander-Bloch, A. F., Shinohara, R. T., Raznahan, A., Gur, R. E., Gur, R. C., Bassett, D. S., & Satterthwaite, T. D. (2020). Development of structure–function coupling in human brain networks during youth. *Proceedings of the National Academy of Sciences*, *117*(1), 771–778. https://doi.org/10.1073/pnas.1912034117

Chan, M. Y., Park, D. C., Savalia, N. K., Petersen, S. E., & Wig, G. S. (2014). Decreased segregation of brain systems across the healthy adult lifespan. *Proceedings of the National Academy of Sciences*, *111*(46), Article 46. https://doi.org/10.1073/pnas.1415122111

Dhollander, T., Mito, R., Raffelt, D., & Connelly, A. (2019). Improved white matter response function estimation for 3-tissue constrained spherical deconvolution. *Proceedings of the 27th Annual Meeting of the International Society of Magnetic Resonance in Medicine*, 555. https://archive.ismrm.org/2019/0555.html

Dhollander, T., Raffelt, D., & Connelly, A. (2016). A novel iterative approach to reap the benefits of multi-tissue CSD from just single-shell (+b=0) diffusion MRI data. *Proceedings of the 24th Annual Meeting of the International Society of Magnetic Resonance in Medicine*. International Society of Magnetic Resonance in Medicine. https://archive.ismrm.org/2016/3010.html

Ewers, M., Luan, Y., Frontzkowski, L., Neitzel, J., Rubinski, A., Dichgans, M., Hassenstab, J., Gordon, B. A., Chhatwal, J. P., Levin, J., Schofield, P., Benzinger, T. L. S., Morris, J. C.,

Goate, A., Karch, C. M., Fagan, A. M., McDade, E., Allegri, R., Berman, S., … Franzmeier, N. (2021). Segregation of functional networks is associated with cognitive resilience in Alzheimer's disease. *Brain*, *144*(7), 2176–2185. https://doi.org/10.1093/brain/awab112

Ferreira, L. K., Lindberg, O., Santillo, A. F., & Wahlund, L.-O. (2022). Functional connectivity in behavioral variant frontotemporal dementia. *Brain and Behavior*, *12*(12), Article 12. https://doi.org/10.1002/brb3.2790

Filippi, M., Basaia, S., Canu, E., Imperiale, F., Meani, A., Caso, F., Magnani, G., Falautano, M., Comi, G., Falini, A., & Agosta, F. (2017). Brain network connectivity differs in early-onset neurodegenerative dementia. *Neurology*, *89*(17), 1764–1772. https://doi.org/10.1212/WNL.0000000000004577

Garyfallidis, E., Brett, M., Amirbekian, B., Rokem, A., Van Der Walt, S., Descoteaux, M., & Nimmo-Smith, I. (2014). Dipy, a library for the analysis of diffusion MRI data. *Frontiers in Neuroinformatics*, *8*. https://doi.org/10.3389/fninf.2014.00008

Godefroy, V., Batrancourt, B., Charron, S., Bouzigues, A., Bendetowicz, D., Carle, G., Rametti-Lacroux, A., Bombois, S., Cognat, E., Migliaccio, R., & Levy, R. (2022). Functional connectivity correlates of reduced goal-directed behaviors in behavioural variant frontotemporal dementia. *Brain Structure & Function*, *227*(9), 2971–2989. https://doi.org/10.1007/s00429-022-02519-5

Gorgolewski, K., Burns, C. D., Madison, C., Clark, D., Halchenko, Y. O., Waskom, M. L., & Ghosh, S. S. (2011). Nipype: A flexible, lightweight and extensible neuroimaging data processing framework in python. *Frontiers in Neuroinformatics*, *5*. https://doi.org/10.3389/fninf.2011.00013

Goulden, N., Khusnulina, A., Davis, N. J., Bracewell, R. M., Bokde, A. L., McNulty, J. P., & Mullins, P. G. (2014). The salience network is responsible for switching between the default mode network and the central executive network: Replication from DCM. *NeuroImage*, *99*, 180–190. https://doi.org/10.1016/j.neuroimage.2014.05.052

He, L., Wang, X., Zhuang, K., & Qiu, J. (2020). Decreased dynamic segregation but increased dynamic integration of the resting-state functional networks during normal aging. *Neuroscience*, *437*, 54–63. https://doi.org/10.1016/j.neuroscience.2020.04.030

Honey, C. J., Thivierge, J.-P., & Sporns, O. (2010). Can structure predict function in the human brain? *NeuroImage*, *52*(3), 766–776. https://doi.org/10.1016/j.neuroimage.2010.01.071

Kellner, E., Dhital, B., Kiselev, V. G., & Reisert, M. (2016). Gibbs-ringing artifact removal based on local subvoxel-shifts. *Magnetic Resonance in Medicine*, *76*(5), 1574–1581. https://doi.org/10.1002/mrm.26054

Lagarde, J., Valabrègue, R., Corvol, J.-C., Pineau, F., Le Ber, I., Vidailhet, M., Dubois, B., & Levy, R. (2013). Are frontal cognitive and atrophy patterns different in PSP and bvFTD? A comparative neuropsychological and VBM Study. *PLoS ONE*, *8*(11), e80353. https://doi.org/10.1371/journal.pone.0080353

Lezak, M. D., Howieson, D. B., Bigler, E. D., & Tranel, D. (2012). *Neuropsychological assessment* (5th ed., pp. xxv, 1161). Oxford University Press.

Menon, V., & Uddin, L. Q. (2010). Saliency, switching, attention and control: A network model of insula function. *Brain Structure & Function*, *214*(5–6), 655–667. https://doi.org/10.1007/s00429-010-0262-0

Mowinckel, A. M., & Vidal-Piñeiro, D. (2020). Visualization of brain statistics with R packages ggseg and ggseg3d. *Advances in Methods and Practices in Psychological Science*, *3*(4), 466–483. https://doi.org/10.1177/2515245920928009

Power, J. D., Mitra, A., Laumann, T. O., Snyder, A. Z., Schlaggar, B. L., & Petersen, S. E. (2014). Methods to detect, characterize, and remove motion artifact in resting state fMRI. *NeuroImage*, *84*, 320–341. https://doi.org/10.1016/j.neuroimage.2013.08.048

Raffelt, D. A., Tournier, J.-D., Smith, R. E., Vaughan, D. N., Jackson, G., Ridgway, G. R., & Connelly, A. (2017). Investigating white matter fibre density and morphology using fixel-based analysis. *NeuroImage*, *144*(Pt A), 58–73. https://doi.org/10.1016/j.neuroimage.2016.09.029

Rascovsky, K., Hodges, J. R., Knopman, D., Mendez, M. F., Kramer, J. H., Neuhaus, J., van Swieten, J. C., Seelaar, H., Dopper, E. G. P., Onyike, C. U., Hillis, A. E., Josephs, K. A., Boeve, B. F., Kertesz, A., Seeley, W. W., Rankin, K. P., Johnson, J. K., Gorno-Tempini, M.-L., Rosen, H., … Miller, B. L. (2011). Sensitivity of revised diagnostic criteria for the behavioural variant of frontotemporal dementia. *Brain*, *134*(9), 2456–2477. https://doi.org/10.1093/brain/awr179

Rittman, T., Borchert, R., Jones, S., van Swieten, J., Borroni, B., Galimberti, D., Masellis, M., Tartaglia, M. C., Graff, C., Tagliavini, F., Frisoni, G. B., Laforce, R., Finger, E., Mendonça, A., Sorbi, S., Rohrer, J. D., Rowe, J. B., Afonso, S., Almeida, M. R., … Zulaica, M. (2019). Functional network resilience to pathology in presymptomatic genetic frontotemporal dementia. *Neurobiology of Aging*, *77*, 169–177. https://doi.org/10.1016/j.neurobiolaging.2018.12.009

Schaefer, A., Kong, R., Gordon, E. M., Laumann, T. O., Zuo, X.-N., Holmes, A. J., Eickhoff, S. B., & Yeo, B. T. T. (2018). Local-global parcellation of the human cerebral cortex from intrinsic functional connectivity MRI. *Cerebral Cortex*, *28*(9), 3095–3114. https://doi.org/10.1093/cercor/bhx179

Schilling, K. G., Blaber, J., Huo, Y., Newton, A., Hansen, C., Nath, V., Shafer, A. T., Williams, O., Resnick, S. M., Rogers, B., Anderson, A. W., & Landman, B. A. (2019). Synthesized b0 for diffusion distortion correction (Synb0-DisCo). *Magnetic Resonance Imaging*, *64*, 62–70. https://doi.org/10.1016/j.mri.2019.05.008

Seeley, W. W. (2019). The salience network: A neural system for perceiving and responding to homeostatic demands. *Journal of Neuroscience*, *39*(50), 9878–9882. https://doi.org/10.1523/JNEUROSCI.1138-17.2019

Seeley, W. W., Crawford, R. K., Zhou, J., Miller, B. L., & Greicius, M. D. (2009). Neurodegenerative diseases target large-scale human brain networks. *Neuron*, *62*(1), Article 1. https://doi.org/10.1016/j.neuron.2009.03.024

Seltman, R. E., & Matthews, B. R. (2012). Frontotemporal Lobar Degeneration. *CNS Drugs*, *26*(10), 841–870. https://doi.org/10.2165/11640070-000000000-00000

Smith, R. E., Tournier, J.-D., Calamante, F., & Connelly, A. (2013). SIFT: Spherical-deconvolution informed filtering of tractograms. *NeuroImage*, *67*, 298–312. https://doi.org/10.1016/j.neuroimage.2012.11.049

Tartaglia, M. C., Zhang, Y., Racine, C., Laluz, V., Neuhaus, J., Chao, L., Kramer, J., Rosen, H., Miller, B., & Weiner, M. (2012). Executive dysfunction in frontotemporal dementia is related to abnormalities in frontal white matter tracts. *Journal of Neurology*, *259*(6), 1071–1080. https://doi.org/10.1007/s00415-011-6300-x

Toller, G., Brown, J., Sollberger, M., Shdo, S. M., Bouvet, L., Sukhanov, P., Seeley, W. W., Miller, B. L., & Rankin, K. P. (2018). Individual differences in socioemotional sensitivity are an index of salience network function. *Cortex*, *103*, 211–223. https://doi.org/10.1016/j.cortex.2018.02.012

Toller, G., Yang, W. F. Z., Brown, J. A., Ranasinghe, K. G., Shdo, S. M., Kramer, J. H., Seeley, W. W., Miller, B. L., & Rankin, K. P. (2019). Divergent patterns of loss of interpersonal warmth in frontotemporal dementia syndromes are predicted by altered intrinsic network connectivity. *NeuroImage: Clinical*, *22*, 101729. https://doi.org/10.1016/j.nicl.2019.101729

Tournier, J.-D., Calamante, F., Gadian, D. G., & Connelly, A. (2004). Direct estimation of the fiber orientation density function from diffusion-weighted MRI data using spherical deconvolution. *NeuroImage*, *23*(3), 1176–1185. https://doi.org/10.1016/j.neuroimage.2004.07.037

Tournier, J.-D., Smith, R., Raffelt, D., Tabbara, R., Dhollander, T., Pietsch, M., Christiaens, D., Jeurissen, B., Yeh, C.-H., & Connelly, A. (2019). MRtrix3: A fast, flexible and open software framework for medical image processing and visualisation. *NeuroImage*, *202*, 116137. https://doi.org/10.1016/j.neuroimage.2019.116137

Tournier, J.-D., Yeh, C.-H., Calamante, F., Cho, K.-H., Connelly, A., & Lin, C.-P. (2008). Resolving crossing fibres using constrained spherical deconvolution: Validation using diffusion-weighted imaging phantom data. *NeuroImage*, *42*(2), 617–625. https://doi.org/10.1016/j.neuroimage.2008.05.002

Trojsi, F., Esposito, F., de Stefano, M., Buonanno, D., Conforti, F. L., Corbo, D., Piccirillo, G., Cirillo, M., Monsurrò, M. R., Montella, P., & Tedeschi, G. (2015). Functional overlap and

divergence between ALS and bvFTD. *Neurobiology of Aging*, *36*(1), 413–423. https://doi.org/10.1016/j.neurobiolaging.2014.06.025

Tustison, N. J., Avants, B. B., Cook, P. A., Zheng, Y., Egan, A., Yushkevich, P. A., & Gee, J. C. (2010). N4ITK: Improved N3 Bias Correction. *IEEE Transactions on Medical Imaging*, *29*(6), 1310–1320. IEEE Transactions on Medical Imaging. https://doi.org/10.1109/TMI.2010.2046908

Tustison, N. J., Cook, P. A., Klein, A., Song, G., Das, S. R., Duda, J. T., Kandel, B. M., van Strien, N., Stone, J. R., Gee, J. C., & Avants, B. B. (2014). Large-scale evaluation of ANTs and FreeSurfer cortical thickness measurements. *NeuroImage*, *99*, 166–179. https://doi.org/10.1016/j.neuroimage.2014.05.044

Veraart, J., Novikov, D. S., Christiaens, D., Ades-aron, B., Sijbers, J., & Fieremans, E. (2016). Denoising of diffusion MRI using random matrix theory. *NeuroImage*, *142*, 394–406. https://doi.org/10.1016/j.neuroimage.2016.08.016

Wang, R., Liu, M., Cheng, X., Wu, Y., Hildebrandt, A., & Zhou, C. (2021). Segregation, integration, and balance of large-scale resting brain networks configure different cognitive abilities. *Proceedings of the National Academy of Sciences*, *118*(23), Article 23. https://doi.org/10.1073/pnas.2022288118

Weintraub, S., Besser, L., Dodge, H. H., Teylan, M., Ferris, S., Goldstein, F. C., Giordani, B., Kramer, J., Loewenstein, D., Marson, D., Mungas, D., Salmon, D., Welsh-Bohmer, K., Zhou, X.-H., Shirk, S. D., Atri, A., Kukull, W. A., Phelps, C., & Morris, J. C. (2018). Version 3 of the Alzheimer Disease Centers' neuropsychological test battery in the Uniform Data Set (UDS). *Alzheimer Disease & Associated Disorders*, *32*(1), 10–17. https://doi.org/10.1097/WAD.0000000000000223

Weintraub, S., Salmon, D., Mercaldo, N., Ferris, S., Graff-Radford, N. R., Chui, H., Cummings, J., DeCarli, C., Foster, N. L., Galasko, D., Peskind, E., Dietrich, W., Beekly, D. L., Kukull, W. A., & Morris, J. C. (2009). The Alzheimer's Disease Centers' Uniform Data Set (UDS): The neuropsychological test battery. *Alzheimer Disease and Associated Disorders*, *23*(2), 91–101. https://doi.org/10.1097/WAD.0b013e318191c7dd

Yeo, B. T. T., Krienen, F. M., Sepulcre, J., Sabuncu, M. R., Lashkari, D., Hollinshead, M., Roffman, J. L., Smoller, J. W., Zöllei, L., Polimeni, J. R., Fischl, B., Liu, H., & Buckner, R. L. (2011). The organization of the human cerebral cortex estimated by intrinsic functional connectivity. *Journal of Neurophysiology*, *106*(3), 1125–1165. https://doi.org/10.1152/jn.00338.2011